



# Lithium recovery from brines by lithium membrane flow capacitive deionization (Li-MFCDI) – A proof of concept

H.M. Saif, J.G. Crespo, S. Pawlowski\*

LAQV-REQUIMTE, DQ, FCT, Universidade NOVA de Lisboa, 2829-516 Caparica, Portugal

## ARTICLE INFO

### Keywords:

Lithium  
Brines  
Lithium selective membranes  
Flow capacitive deionization  
3D printing

## ABSTRACT

The demand of lithium for electric vehicles and energy storage devices is increasing rapidly, thus new sources of lithium (such as seawater and natural or industrial brines), as well as sustainable methods for its recovery, will need to be explored/developed soon. This work presents a novel electromembrane process, called Lithium Membrane Flow Capacitive Deionization (Li-MFCDI), which was tested to recover lithium from a synthetic geothermal brine containing a much higher mass concentration of sodium than lithium (more than 650 times). Specifically, a ceramic lithium-selective membrane was integrated into a flow capacitive deionization (FCDI) cell, which was specifically designed, and 3D printed, to allow simultaneous charging and regeneration of the employed flow electrodes. Despite the extremely high  $\text{Na}^+/\text{Li}^+$  mass ratio in the feed stream, 99.98% of the sodium was rejected and the process selectivity for lithium over other monovalent cations was  $141 \pm 5.85$  for  $\text{Li}^+/\text{Na}^+$  and  $46 \pm 1.46$  for  $\text{Li}^+/\text{K}^+$ . The Li-MFCDI process exhibited a stable behaviour over a 7-day test period, and the estimated energy consumption was  $16.70 \pm 1.63$  kWh/kg of  $\text{Li}^+$  recovered in the draw solution. These results demonstrate promising potential of the Li-MFCDI for the sustainable lithium recovery from saline streams.

## Introduction

Lithium has emerged as a critical raw material due to its use in lithium-ion batteries, which are necessary for electric vehicles, the renewable energy sector, and portable electronic devices. The global demand for lithium has increased significantly, and it is projected to reach 1.4–1.7 Mtons by 2030, up from 0.54 Mtons in 2021 (Swain, 2017; Yang et al., 2018; Bhutada, 2023). Traditionally, lithium is extracted from land-based resources like salt-lake brines and high-grade ores using a chemical precipitation process that involves evaporation ponds, chemicals and water, making it pollution-intensive and time-consuming (Vikström et al., 2013). Furthermore, lithium land reserves, beside expected to be depleted by 2080 (Yang et al., 2018), are unevenly distributed with approximately 65% located in South America (Vikström et al., 2013; Grosjean et al., 2012). An alternative and sustainable source of lithium might be the world ocean, with an estimated 230 billion tons of lithium available, although the low lithium concentration in it (0.1–0.2 mg/L) can make its recovery challenging (Choubey et al., 2017). Thus, industrial or natural brines, such as seawater reverse osmosis brines, bitterns formed after extracting table salt from seawater or geothermal brines, with higher concentrations of lithium (2–20

mg/L), seems to be more attractive sources for lithium extraction (Siekierka et al., 2018; Vicari et al., 2022; Cipollina et al., 2022).

Electromembrane processes such as electrodialysis (ED), capacitive deionization (CDI) or flow capacitive deionization (FCDI) are commonly used for desalination of saline streams, thus without targeting any specific ion (Al-Amshawee et al., 2020; Porada et al., 2013; Jeon et al., 2013). These processes have an advantage over other separation techniques as their driving force is electricity which can be generated from renewable energy sources. This is particularly relevant in the context of Sustainable Development Goals and EU electrification strategy under the European Green Deal (European Commission 2023). Among them, FCDI, which is the most recent technology (proposed in 2013), uses flow electrodes (carbon slurries) to remove ions from saline water based on the electro-sorption principle (Jeon et al., 2013). Flow electrodes can be recirculated and regenerated in a loop arrangement between cathode and anode, which allows to increase salts removal and to make the process continuous and energetically efficient (Yang et al., 2021). However, selective recovery of specific ions, such as lithium, by FCDI has not been explored yet. Thus, there is a huge potential for FCDI improvement, for example, by incorporation of membranes with functionalised selectivity towards a specific ion (Saif et al., 2021). In this

\* Corresponding author.

E-mail address: [s.pawlowski@fct.unl.pt](mailto:s.pawlowski@fct.unl.pt) (S. Pawlowski).

<https://doi.org/10.1016/j.memlet.2023.100059>

Received 6 July 2023; Received in revised form 25 July 2023; Accepted 9 August 2023

Available online 12 August 2023

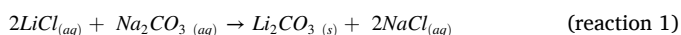
2772-4212/© 2023 The Authors. Published by Elsevier B.V. This is an open access article under the CC BY-NC-ND license (<http://creativecommons.org/licenses/by-nc-nd/4.0/>).

work, a lithium selective membrane was incorporated into a built-in house FCDI stack, and a proof of concept of a lithium membrane flow capacitive deionization (Li-MFCDI) was successfully demonstrated by extracting lithium from a synthetic geothermal brine with ~650 times more sodium than lithium.

### Lithium membrane flow capacitive deionization (Li-MFCDI) concept

A lithium membrane flow capacitive deionization cell (Li-MFCDI) consists of anion exchange membranes and lithium selective membranes stacked alternately between current collectors with flow electrode channels. Fig. 1 shows a cell with one feed channel, one draw channel, and cathodic and anodic flow electrode channels.

As in any electromembrane desalination process, cations and anions migrate toward cathode and anode, respectively. The anion exchange membranes block transport of cations, while lithium selective membranes should only allow for transport of lithium, while blocking transport of anions and of other cations. In this particular case, the central membrane is a lithium selective one, while the membranes at the vicinity of current collectors are anion exchange ones, but an opposite arrangement is also possible. Thus, using this arrangement, the lithium is removed from the feed directly through the lithium selective membrane to the draw solution, while anions migrate to the anodic flow electrode compartment, at which they adsorb on the surface of the activated carbon. Since the flow electrode circulates in a closed loop between anode and cathode, the activated carbon charged with anions flows to the cathodic compartment, where the anions desorb and migrate to the draw solution. In such a way the electroneutrality conditions at the feed and draw solution are maintained, while the driving force continues constant overtime due to on-site regeneration of flow electrodes. Afterwards, the lithium from the enriched draw solution can be converted, if required, into lithium carbonate by the following reaction (Cipollina et al., 2022; Kelly et al., 2021; Chordia et al., 2022).



### Materials and methods

#### Materials

Lithium chloride (99% purity, Alfa Aesar), sodium chloride (99.9% purity, Sigma-Aldrich), potassium chloride (99.5% purity, Sigma-Aldrich) and magnesium chloride (99% purity, Sigma-Aldrich) were used as received to prepare the feed solution (synthetic geothermal

brine). The draw solution was prepared by using hydrochloric acid (37% w/w, Sigma-Aldrich). YP50F activated carbon (Chemviron, Germany), usually employed at electric double layer capacitors, was used to prepare flow electrode slurry. A Lithium ion conducting glass ceramic membrane (LICGC AG-01 from OHARA corporation, Japan) was used as a lithium selective membrane (LiSM). The LiSM membrane was circular, with 50.8 mm diameter and 0.25 mm thickness. FAB-PK-130 membranes (Fumatech, Germany) were used as anion exchange membranes. Graphite plates (10 × 10 × 1 cm from Graphite technologies, Portugal) were used to prepare the current collectors. Polyethylene glycol (PET-G) (Dowire, Portugal) and Flexfill Thermoplastic elastomer TPE 90A 1.75 mm filaments (Filamentum, Czech Republic) were used to 3D print different parts of the Li-MFCDI cell. Plexiglass plates (10 × 10 × 1.5 cm) were used as end plates of the Li-MFCDI cell.

#### Li-MFCDI cell assembly

Li-MFCDI cell (Fig. 2) was constructed in-house by using a ZMorph VX Multitool 3D printer (Zmorph3D, Poland).

Computerized numerical control (CNC) milling toolhead with a 1 mm bit was used to engrave serpentine channels (dimensions: length 275 mm, width 2 mm, depth 2 mm) on graphite plates to prepare current collectors. The anion exchange membranes were placed in front of both graphite current collectors. A rubber sheet (1 mm thick), cut with a laser toolhead, was used as a gasket between the anion exchange membrane and the feed and draw solution compartments to avoid leakages. The feed and draw compartments were printed with a 0.3 mm nozzle using a PET-G filament. The nozzle and bed temperature for PET-G printing were 230 °C and 80 °C, respectively. The volume of feed and receiver compartment was 16 mL. A LICGC AG-01 membrane was used as lithium selective membrane (LiSM) due to its very high lithium-ion conductivity  $1 \times 10^{-4}$  S/cm at room temperature (OHARA Corporation 2023). The lithium ion conduction mechanism of LICGC AG-01, proposed by the manufacturer (OHARA Corp. Japan), is vacancy diffusion where lithium ions fill the lattice cavities and leave behind a vacancy for upcoming lithium ions. The LICGC AG-01 has a crystal structure with a lattice cavity size similar to the ionic lithium size which should only allow lithium ions to pass and hinder all other ions. The active area of LiSM in the cell was 10.75 cm<sup>2</sup>. TPE filament was used to print the O-rings applied to fix LiSM between the feed and the receiver compartment. The nozzle and bed temperature for TPE printing were 245 °C and 60 °C, respectively. The thickness of O-rings was 1 mm with internal and external diameter of 37.0 and 50.8 mm, respectively. All the assembly was stacked between two plexiglass endplates. Before starting the experiments, deionized water was circulated through the cell for several

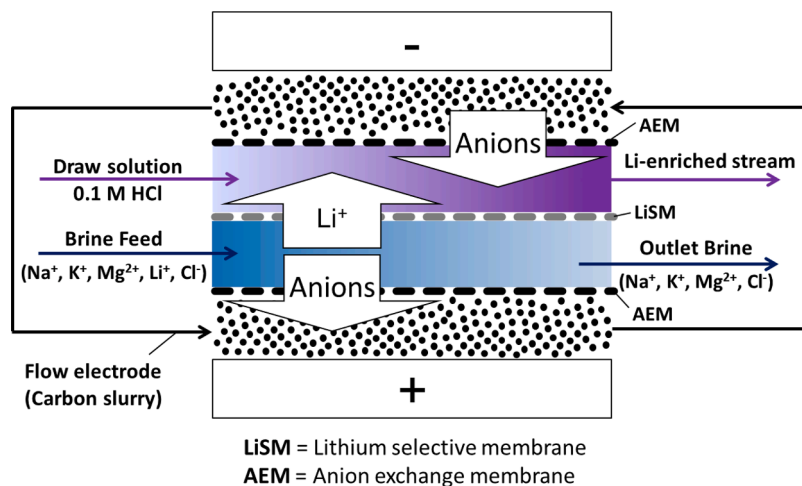


Fig. 1. Lithium membrane flow capacitive deionization (Li-MFCDI) concept with lithium selective membrane (LiSM) separating draw and feed solutions, and anion exchange membranes (AEMs) at the vicinity of current collectors.

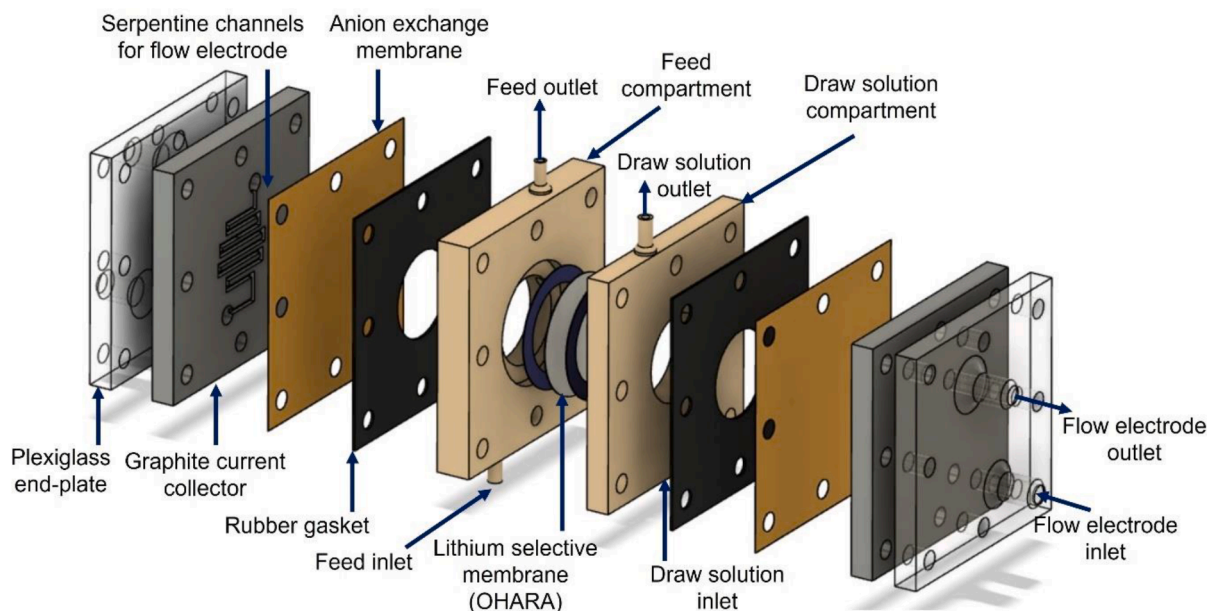


Fig. 2. Schematic representation of the lithium membrane flow capacitive deionization (Li-MFCDI) cell used in this study.

hours to ensure that there are no leakages. The 3D printed parts of the Li-MFCDI cell are shown in Fig. SI.1 in the Supplementary Information.

#### Preparation of flow electrode, feed and receiver solutions

YP50F activated carbon was used to prepare the flow electrode slurry. YP50F was chosen due its high specific surface area (1600 m<sup>2</sup>/g calculated by Brunauer–Emmett–Teller (BET) method) available for ion adsorption and desorption (Porada et al., 2014a; b). Therefore, a 10 wt.% YP50F slurry was prepared by adding 20 g of YP50F into 180 g of a 1 g/L NaCl solution. The mixture was stirred for 24 h to obtain a homogeneous carbon suspension. Lithium, sodium, potassium, and magnesium chloride salts were used to prepare 2 L of feed, mimicking the composition of a geothermal brine (Table 1) (Siekierka et al., 2018). As a draw solution, 0.2 L of a 0.1 M HCl solution was prepared from 37% (w/w) HCl solution.

#### Recovery of lithium from synthetic geothermal brine by Li-MFCDI

The Li-MFCDI cell was operated for 7 days as it is schematically illustrated in Fig. 3.

The feed and draw solutions were recirculated at a flow rate of 10 mL/min which correspond to the residence time of 96 s. The flow electrode was recirculated at the flow rate of 100 mL/min which correspond to the residence time of 0.66 s. A Masterflex standard digital drive (model no: 07,522–20) with a four channel pump head (model no: 7536–04), Viton tubing size 15 (4.8 mm internal diameter) were used for circulation of flow electrodes. Two peristaltic pumps (Leadfluid drive mode no: BT100S with YT15 pump head, silicon tubing size 15 (4.8 mm internal diameter)) were used for feed and draw solutions' circulation. The Li-MFCDI experiment was conducted at constant voltage mode by applying a potential of 1.2 V using a Vertex 5A potentiostat (Ivium Technologies, The Netherlands). The composition of feed and draw solutions was assessed by inductively coupled plasma atomic emission spectroscopy (ICP-AES) Horiba Jobin-Yvon, France, Ultima model. The

Table 1  
Composition of the feed solution simulating a synthetic geothermal brine.

Na <sup>+</sup> (g/L)	Li <sup>+</sup> (g/L)	K <sup>+</sup> (g/L)	Mg <sup>2+</sup> (g/L)	Cl <sup>-</sup> (g/L)
10.298	0.0157	0.102	0.050	16.192

draw solution samples (4 mL each) were taken at 0, 0.5, 1.5, 3, 6, 24, 48, 72, 96, 120, 144, and 168 h. The feed composition was analysed at the start and at the end of the experiment.

The molar ionic fluxes between feed and draw solution compartments were calculated using Eq. (1).

$$\text{Molar ionic } (M^{i+}) \text{ flux } \left( \frac{\text{mol}}{\text{m}^2 \cdot \text{h}} \right) = \frac{[M^{i+}]_{t=t}^D \times V_D}{A \times t}, \quad (1)$$

where  $M^{i+}$  can be Li<sup>+</sup> or Na<sup>+</sup> or K<sup>+</sup> or Mg<sup>2+</sup>, and  $i$  is the valence state of each ion,  $[M^{i+}]_{t=t}^D$  is the molar ionic concentration of  $M^{i+}$  ion in draw solution (mol/L) at a time  $t$  (h),  $V_D$  is the volume of draw solution (L) and  $A$  is the membrane's active area (m<sup>2</sup>).

The rejection of each ion was calculated using Eq. (2) (Hoshino, 2013).

$$\text{Ion } (M^{i+}) \text{ rejection } (\%) = \left( 1 - \frac{[M^{i+}]_{t=t}^D \times V_D}{[M^{i+}]_{t=0}^F \times V_F} \right) \times 100, \quad (2)$$

where  $[M^{i+}]_{t=0}^F$  is the molar ionic concentration of  $M^{i+}$  ion in feed solution at time  $t = 0$  h and  $V_F$  is the volume of feed solution (L).

Lithium selectivity, defined as the ratio of enrichment in lithium against enrichment of other competing cations (sodium, potassium or magnesium) was calculated according to Eq. (3):

$$S_{\text{Li}^+/\text{M}^{i+}} = \frac{[\text{Li}^+]_{t=t}^D / [\text{Li}^+]_{t=0}^F}{[M^{i+}]_{t=t}^D / [M^{i+}]_{t=0}^F}, \quad (3)$$

where  $[\text{Li}^+]_{t=0}^F$  is the initial molar ionic concentration of lithium in the feed.

The consumed energy  $E$  (W.s) was calculated by multiplying the charge  $Q$  (C) which was transferred, and the applied voltage  $V$  (V) as described by Eq. (4) (Morita et al., 2022):

$$E = Q \times V, \quad (4)$$

where  $V$  was 1.2 V, as the Li-MFCDI cell was operated at constant voltage mode. The transferred charge was calculated from the experimental chronoamperometric curve, after achieving a plateau (thus stable operation conditions), by its integration over time as described by Eq. (5):

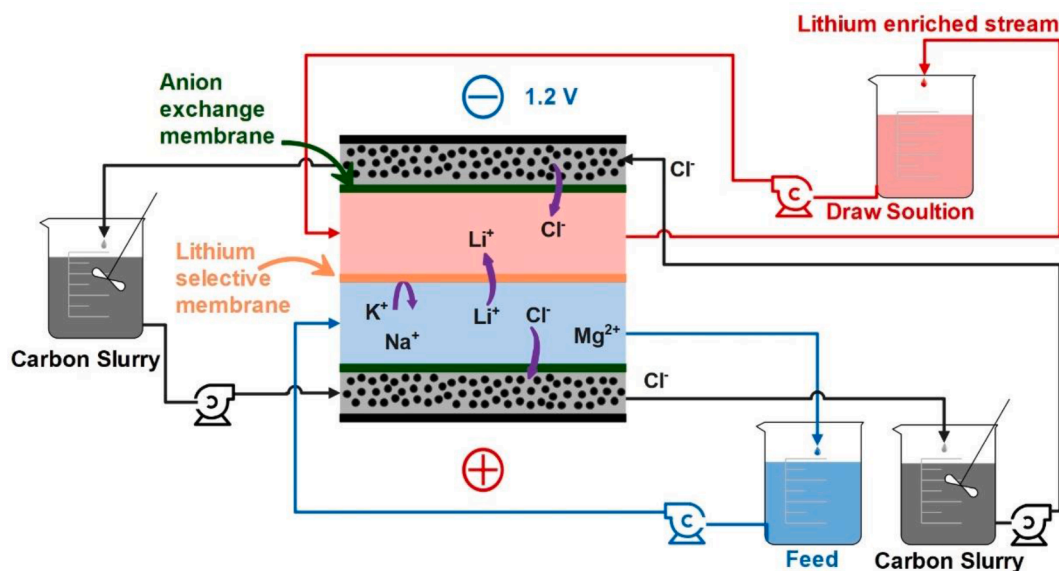


Fig. 3. A schematic layout of lithium recovery by lithium membrane flow capacitive deionization (Li-MFCDDI).

$$Q = \int_0^t I(t) dt \quad (5)$$

where  $I(t)$  is the instantaneous current value (A).

## Results and discussion

The current passing through the Li-MFCDDI was stable over almost all the period of operation (7 days) as can be seen in Fig. SI.2a in the Supplementary Information. Only during the first two hours of the test a sharp current drop from 0.21 to 0.05 mA occurred, most probably due to an initial adsorption of ions on pristine flow electrodes. From that point on, the average current value was stable around 0.05 mA. As mentioned earlier, the employed lithium selective membrane was a dense ceramic membrane, without any fixed charges usually present in polymeric ion-exchange membranes, which might explain the relatively low current value.

Fig. 4a shows the ionic concentrations in the draw solution over time. As desired, the lithium concentration in the draw solution increased with time, although the concentration of other cations also increased and, in particular, the one of sodium due to the remarkably high  $\text{Na}^+/\text{Li}^+$  ratio in the feed. As a result, some  $\text{Na}^+$  ions successfully competed against  $\text{Li}^+$  ions and crossed through the LiSM.

Nevertheless, the molar ionic flux of  $\text{Li}^+$  was similar to the flux of  $\text{Na}^+$  (Fig. S.2b), confirming the high selectivity towards  $\text{Li}^+$  since 99.98% of sodium was rejected. This achievement is particularly important as one of the main challenges when recovering lithium from saline streams is the presence of sodium, which is a hard task since both ions are monovalent, and the sodium is usually present at much higher quantity than lithium (in this case study the  $\text{Na}^+/\text{Li}^+$  mass ratio in the feed was more than 650). The decreasing trend of ionic fluxes is expectable by the fact the operation was performed in a batch mode. It was also noted that the employed LiSM did not totally hinder the  $\text{Mg}^{2+}$  ion, which might be caused by the similar ionic radii of  $\text{Li}^+$  [0.6 Å] and  $\text{Mg}^{2+}$  [0.65 Å] (Geise et al., 2014). Using a monovalent cation exchange membrane or alternatively, a crystallizer reactor (Battaglia et al., 2022), to remove first the divalent cations such as  $\text{Mg}^{2+}$  from the feed before going to the lithium recovery unit, might further optimize lithium extraction. Nonetheless, selectivity values much higher than 1 were achieved:  $141 \pm 5.85$  for  $\text{Li}^+/\text{Na}^+$ ,  $46 \pm 1.46$  for  $\text{Li}^+/\text{K}^+$  and  $3 \pm 0.22$  for  $\text{Li}^+/\text{Mg}^{2+}$  at the end of the 7-day operation (Fig. 4b), as well as during all operation period

(Fig. SI.2c in the Supplementary Information) which is a very promising starting point for further Li-MFCDDI optimization. Moreover, pH values in the draw solution were also monitored during the 7-day test (Fig. SI.2d in the Supplementary Information) and no significant variation was observed.

Furthermore, when comparing herein obtained results with other works focused on lithium recovery, the Li-MFCDDI allowed for a relatively fast selective recovery of lithium due to recirculation of the conductive carbon flow electrodes, which minimize the electrical resistance of the cell and kept the driving force constant due to their regeneration onsite. For comparison, Hoshino (Hoshino, 2015), performed an electro dialysis experiment for 72 h using seawater as a feed and the same LiSM used in this study, and the average current value was  $2.7 \times 10^{-5}$  mA, which is 1860 times less than the one obtained herein at Li-MFCDDI.

Regarding the energy expenditure for the Li-MFCDDI,  $16.70 \pm 1.63$  kWh/(kg of  $\text{Li}^+$  in the draw solution) were necessary, which is less than the energy consumption reported by Li et al. (Li et al., 2021) where 76.34 kWh were required to extract 1 kg of lithium from seawater. Furthermore, considering an electricity cost of 0.2104 €/kWh for non-household electricity consumers in the EU, in the second half of 2022 (Eurostat 2023),  $16.70 \pm 1.63$  kWh costs only  $3.51 \pm 0.34$  €, which is less than 1% of the commercial value of the lithium carbonate (when considering its price in November 2022, 78.85 €/kg of  $\text{Li}_2\text{CO}_3$  (Trading Economics 2023)) which may be produced in a posterior crystallization step (reaction 1), when assuming a 100% conversion of 1 kg of lithium into 5.32 kg of  $\text{Li}_2\text{CO}_3$ .

## Conclusions

This work presents a novel electromembrane method, lithium-membrane flow capacitive deionization (Li-MFCDDI), for lithium recovery from saline streams. The Li-MFCDDI cell can easily be constructed, as it can be manufactured using a standard 3D printer. The proof of concept for Li-MFCDDI was successfully validated through a 7-day trial, demonstrating the recovery of lithium from a Na-rich geothermal brine. Remarkably high selectivity values for lithium over sodium and potassium ( $\text{Li}^+/\text{Na}^+ = 141 \pm 5.85$ ,  $\text{Li}^+/\text{K}^+ = 46 \pm 1.46$ ) were achieved, surpassing the challenge of a  $\text{Na}^+/\text{Li}^+$  mass ratio exceeding 650 in the feed solution. Since the driving force of Li-MFCDDI is the electrochemical potential difference, further enhanced by electro-sorption of ions on the surface of activated carbon particles in the flow electrode, there is no

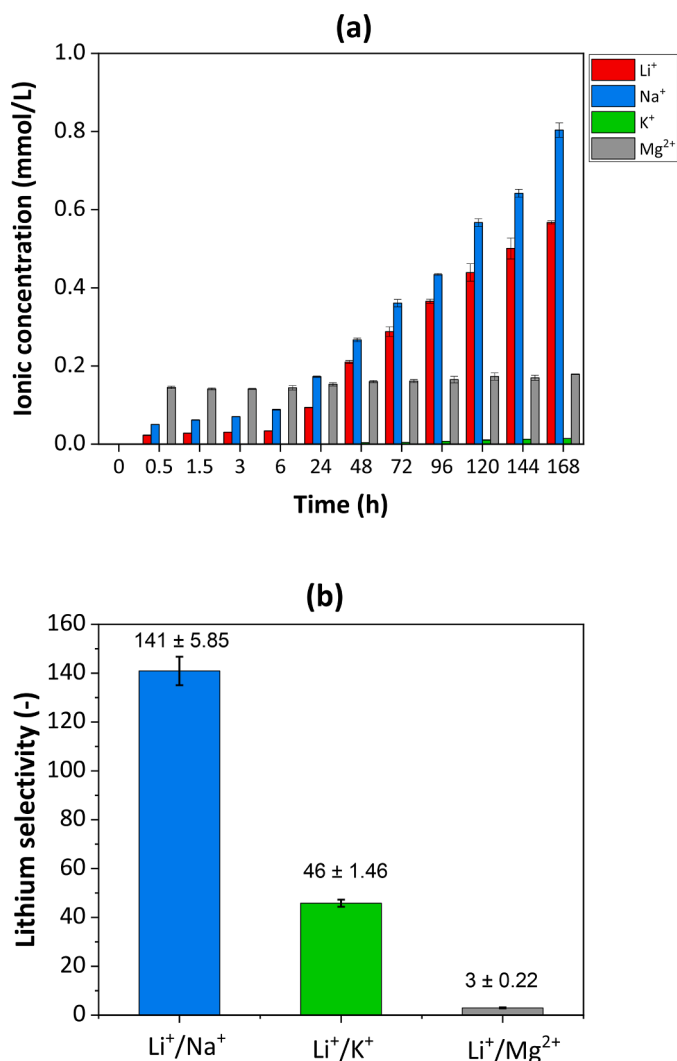


Fig. 4. (a) Concentration of different ions in the draw solution along a 7- day Li-MFCDI cell operation when using a synthetic geothermal brine as the feed; (b) Li-MFCDI selectivity, calculated according to Eq. (3), at the end of the 7- day trial.

need of using harmful chemicals and the release of carbon dioxide is prevented, contributing to the environmentally friendly character of this approach. The successful development and promising performance of Li-MFCDI demonstrate its potential for further optimization and scale-up, which can pave up the way for sustainable utilization of so far unexplored resources of highly saline streams, such as industrial or natural brines.

#### Declaration of Competing Interest

The authors declare that they have no known competing financial interests or personal relationships that could have appeared to influence the work reported in this paper.

#### Data availability

Data will be deposited at Zenodo as part of the SEArcularMINE project, according to FAIR principles.

#### Acknowledgments

This project has received funding from Fundação para a Ciência e Tecnologia (FCT), I.P. under grant agreement no PTDC/EQU-EQU/6193/2020 (Se(L)ect(i)vity) and the European Union Horizon 2020 research and innovation programme under grant agreement no 869467 (SEArcularMINE). This work was also supported by the Associate Laboratory for Green Chemistry – LAQV which is financed by national Portuguese funds from FCT/MCTES (UIDB/50006/2020). Hafiz Muhammad Saif Ullah Saleem acknowledges FCT/MCTES for his PhD grant (2020.09828.BD).

#### Supplementary materials

Supplementary material associated with this article can be found, in the online version, at doi:10.1016/j.memlet.2023.100059.

#### References

- Al-Amshawee, S., Yunus, M.Y.B.M., Azoddein, A.A.M., Hassell, D.G., Dakhil, I.H., Hasan, H.A., 2020. Electrodialysis desalination for water and wastewater: a review. *Chem. Eng. J.* 380, 122231 <https://doi.org/10.1016/j.cej.2019.122231>.
- Battaglia, G., Domina, M.A., Romano, S., Tamburini, A., Cipollina, A., Micale, G., 2022. Magnesium hydroxide nanoparticles production from natural bitterns. *Chem. Eng. Trans.* 96, 43–48. <https://doi.org/10.3303/CET2296008>.
- Bhutada, G., 2023. This chart shows which countries produce the most lithium. <http://www.weforum.org/agenda/2023/01/chart-countries-produce-lithium-world/#:~:text=As%20the%20world%20produces%20more,tonnes%20of%20LCE%20in%202021.> (Accessed May 17, 2023).
- Chordia, M., Wickerts, S., Nordelöf, A., Arvidsson, R., 2022. Life cycle environmental impacts of current and future battery-grade lithium supply from brine and spodumene. *Resour. Conserv. Recycl.* 187, 106634 <https://doi.org/10.1016/j.resconrec.2022.106634>.
- Choubey, P.K., Chung, K.S., seuk Kim, M., chun Lee, J., Srivastava, R.R., 2017. Advance review on the exploitation of the prominent energy-storage element lithium. Part II: from sea water and spent lithium ion batteries (LIBs). *Miner. Eng.* 110, 104–121. <https://doi.org/10.1016/j.mineng.2017.04.008>.
- Cipollina, A., Winter, D., Battaglia, G., Berkemeyer, L., Cortina, J.L., de Labastida, M.F., Rodriguez, J.L., 2022. Recovery of lithium carbonate from dilute Li-rich brine via homogenous and heterogeneous precipitation. *Ind. Eng. Chem. Res.* 61, 13589–13602. <https://doi.org/10.1021/acs.iecr.2c01397>.
- European Commission, Delivering the European green deal, (2023). [https://commission.europa.eu/strategy-and-policy/priorities-2019-2024/european-green-deal/deliverin-g-european-green-deal\\_en](https://commission.europa.eu/strategy-and-policy/priorities-2019-2024/european-green-deal/deliverin-g-european-green-deal_en) (Accessed June 3, 2023).
- Eurostat, Electricity prices for non-household consumers, (2023). [https://ec.europa.eu/eurostat/statistics-explained/index.php?title=Electricity\\_price\\_statistics#Electricity\\_prices\\_for\\_non-household\\_consumers](https://ec.europa.eu/eurostat/statistics-explained/index.php?title=Electricity_price_statistics#Electricity_prices_for_non-household_consumers) (Accessed June 14, 2023).
- Geise, G.M., Paul, D.R., Freeman, B.D., 2014. Fundamental water and salt transport properties of polymeric materials. *Prog. Polym. Sci.* 39, 1–42. <https://doi.org/10.1016/j.progpolymsci.2013.07.001>.
- Grosjean, C., Miranda, P.H., Perrin, M., Poggi, P., 2012. Assessment of world lithium resources and consequences of their geographic distribution on the expected development of the electric vehicle industry. *Renew. Sustain. Energy Rev.* 16, 1735–1744. <https://doi.org/10.1016/j.rser.2011.11.023>.
- Hoshino, T., 2013. Preliminary studies of lithium recovery technology from seawater by electrodialysis using ionic liquid membrane. *Desalination* 317, 11–16. <https://doi.org/10.1016/j.desal.2013.02.014>.
- Hoshino, T., 2015. Innovative lithium recovery technique from seawater by using world-first dialysis with a lithium ionic superconductor. *Desalination* 359, 59–63. <https://doi.org/10.1016/j.desal.2014.12.018>.
- Jeon, S., Park, H., Yeo, J., Yang, S., Cho, C.H., Han, M.H., Kim, D.K., 2013. Desalination via a new membrane capacitive deionization process utilizing flow-electrodes. *Energy Environ. Sci.* 6, 1471–1475. <https://doi.org/10.1039/C3EE24443A>.
- Kelly, J.C., Wang, M., Dai, Q., Winjobi, O., 2021. Energy, greenhouse gas, and water life cycle analysis of lithium carbonate and lithium hydroxide monohydrate from brine and ore resources and their use in lithium ion battery cathodes and lithium ion batteries. *Resour. Conserv. Recycl.* 174, 105762 <https://doi.org/10.1016/j.resconrec.2021.105762>.
- Li, Z., Li, C., Liu, X., Cao, L., Li, P., Wei, R., Li, X., Guo, D., Huang, K.W., Lai, Z., 2021. Continuous electrical pumping membrane process for seawater lithium mining. *Energy Environ. Sci.* 14, 3152–3159. <https://doi.org/10.1039/d1ee00354b>.
- Morita, K., Matsumoto, T., Hoshino, T., 2022. Efficient lithium extraction via electrodialysis using acid-processed lithium-adsorbing lithium lanthanum titanate. *Desalination* 543, 116117. <https://doi.org/10.1016/j.desal.2022.116117>.
- OHARA Corporation, Lithium-ion conducting glass-ceramics (LICGTM), (n.d.). <https://www.oharacorp.com/lic-gc.html> (Accessed June 3, 2023).
- Porada, S., Lee, J., Weingarh, D., Presser, V., 2014a. Continuous operation of an electrochemical flow capacitor. *Electrochem. Commun.* 48, 178–181. <https://doi.org/10.1016/j.elecom.2014.08.023>.

- Porada, S., Weingarh, D., Hamelers, H.V.M., Bryjak, M., Presser, V., Biesheuvel, P.M., 2014b. Carbon flow electrodes for continuous operation of capacitive deionization and capacitive mixing energy generation. *J. Mater. Chem. A Mater.* 2, 9313–9321. <https://doi.org/10.1039/c4ta01783h>.
- Porada, S., Zhao, R., Van Der Wal, A., Presser, V., Biesheuvel, P.M., 2013. Review on the science and technology of water desalination by capacitive deionization. *Prog. Mater. Sci.* 58, 1388–1442. <https://doi.org/10.1016/j.pmatsci.2013.03.005>.
- Saif, H.M., Huertas, R.M., Pawlowski, S., Crespo, J.G., Velizarov, S., 2021. Development of highly selective composite polymeric membranes for Li<sup>+</sup>/Mg<sup>2+</sup> separation. *J. Memb. Sci.* 620, 118891 <https://doi.org/10.1016/j.memsci.2020.118891>.
- Siekierka, A., Tomaszewska, B., Bryjak, M., 2018. Lithium capturing from geothermal water by hybrid capacitive deionization. *Desalination* 436, 8–14. <https://doi.org/10.1016/j.desal.2018.02.003>.
- Swain, B., 2017. Recovery and recycling of lithium: a review. *Sep. Purif. Technol.* 172, 388–403. <https://doi.org/10.1016/j.seppur.2016.08.031>.
- Trading Economics, Lithium carbonate price, (2023). <https://tradingeconomics.com/commodity/lithium> (Accessed June 25, 2023).
- Vicari, F., Randazzo, S., López, J., Fernández de Labastida, M., Vallès, V., Micale, G., Tamburini, A., D'Alì Staiti, G., Cortina, J.L., Cipollina, A., 2022. Mining minerals and critical raw materials from bittern: understanding metal ions fate in saltwork ponds. *Sci. Total Environ.* 847, 157544 <https://doi.org/10.1016/j.scitotenv.2022.157544>.
- Vikström, H., Davidsson, S., Höök, M., 2013. Lithium availability and future production outlooks. *Appl. Energy* 110, 252–266. <https://doi.org/10.1016/j.apenergy.2013.04.005>.
- Yang, F., He, Y., Rosentsvit, L., Suss, M.E., Zhang, X., Gao, T., Liang, P., 2021. Flow-electrode capacitive deionization: a review and new perspectives. *Water Res.* 200, 117222 <https://doi.org/10.1016/j.watres.2021.117222>.
- Yang, S., Zhang, F., Ding, H., He, P., Zhou, H., 2018. Lithium metal extraction from seawater. *Joule* 2, 1648–1651. <https://doi.org/10.1016/j.joule.2018.07.006>.